L E O LIFE TESTING WITH DIFFERENT CHARGE CONTROL

F. Baron
Energy Storage Section
European Space Research and Technology Center
European Space Agency

ABSTRACT

The effect of charge control on the performance of Nickel-Cadmium batteries is very important. The purpose of this paper is to describe the results of three tests performed in the Battery Test Centre of ESTEC. Two techniques were employed: the tapering method well known for space applications, and the temperature derivative technique (TDT) developped by ESTEC.

In addition, a comparative study has been made between the behaviour of a group of 3 batteries charged and discharged in parallel compared to an identical group discharged in parallel, but charged individually.

An approach of evolution laws for the main electrical characteristics of cells is presented, then some ageing equations will be introduced. These tests were supported by the European Space Agency project ERS-1 and analyzed by the University Paul Sabatier of Toulouse (Pr. Comtat) under ESTEC Contract (1).

INTRODUCTION

In ESA GEO Spacecraft, it has become usual to charge the Nickel-Cadmium batteries until a certain temperature-dependent battery voltage has been reached. Following this the battery voltage is held at this value and the current allowed to fall, or "taper". Since the sunlight periods are long compared to the eclipses there is no shortage of time to recharge the batteries. In Low-Earth-Orbit (LEO) the situation is very different, since the battery charging has to be completed within a period of some 65 minutes. With the larger European craft such as SPOT, ERS-1 and EURECA, requiring several kilowatts of eclipse power, it is necessary to minimise the size of the solar array so as to reduce the array and propellant load. In order to use the array power most efficiently it is therefore desirable to reduce to a minimum period of taper charge in which array power is wasted.

Indeed, the tapering method consists in a charge at constant current rate (in general C/2 or C/3) up to an applied battery voltage limit, after which remaining time of charge is performed at constant voltage, the current tapering. For the taper charge control method, eight cell voltage limits spaced 20 mv apart were defined according to the following equation (fig. 3)

$$V_{limit} = 1.372 + (n \times 0.020) - 0.0023\ T$$

Where T is the cell temperature in degree Celsius
      n is the level number

The VL level (n = 5) is chosen in order to maintain the battery fully charged during the life time test; the changes of temperature are automatically compensated with the taper control unit. This method was used for the SPOT tests and the Hybrid tests. At the same time possible alternative criteria indicating battery full charge was considered.

The principle to the new battery charging technique (1) is to terminate the charge at constant current when the battery temperature starts to increase following the endothermic reaction of the first period of charge. The temperature is measured at individual battery cell level at the location of the thin metal thermal conduction plates between the isolated cells. It is thus virtually independent of environmental temperature fluctuations. This technique allows one to reduce by approximately 30% the power compared with the "tapering technique". The logic circuit (figures 4 and 5) detects end of charge during the sunlight phase of an orbit when the battery temperature starts to increase for a temperature derivative level (dT/dt) calculated from the set of thermistors which are connected to the positive input of an operational amplifier set up with a gain of about 2700. The temperature derivative level for end of charge is equal to:

$$dT/dt = dV\ thermistor/dt \times dT/dVth = 0.2\ ^\circ C/hour$$

The remaining part of the sunlight period is spent in open circuit mode. The figures n° 4 and 9 give an example of the relationship between battery voltage, current and cell temperature in a low earth orbit profile.

TEST PROGRAMME

Three tests were conducted as follows, each using the same discharge and available charge time.

1. ('SPOT test') 3 identical batteries charged and discharged in parallel with taper charge control.

2. ('Hybrid test') 3 identical batteries discharged in parallel but charged independently each with taper charge control

3. ('Reference test') A single battery with temperature derivative charge control.

The current passing through each battery of a group was separately measured.

The batteries consist of 14 Ni-Cd cells (SAFT type V035M) connected in series. The nominal capacity is 35 Ah.

Figure 1 shows the method of battery packaging, thermal dissipation being obtained by monitoring the batteries on the ground with an air-cooled baseplate. One cycle consisted of a charge and three steps of discharge chosen to simulate the power profile of the satellite payload (fig. 2).

SYMBOLS AND STUDIED PARAMETERS

A,B,C,D,E,F,G   key points

$\overline{Q_D}$ discharged capacity (average in Ah)

$\overline{Q_C}$ charged capacity (average in Ah)

$\overline{K}$ recharge factor $= \dfrac{\overline{Q_c}}{\overline{Q_d}}$

DOD   depth of discharge
                                (percentage of nominal capacity)

I_C, I_D charge and discharge current (A)

$\overline{U}eoc$ end of charge battery voltage
                                (average over cycling period)

Veoc   end of charge cell voltage (Volt)

$\overline{U}eod$ end of discharge battery voltage
                                (average over cycling period)

W	energie (KJ)

η energie efficiency (percentage) $= \dfrac{W_d}{W_c} \times 100$

σ	standard variation
corr. c	correlation-coefficient

RESULTS ANALYSIS FOR THE SPOT-TESTS (9000 cycles)

A typical record of the battery parameters during one cycle is given with fig. 6. Points of interest are marked by letters.

The parameters of each battery were recorded separately in order to evaluate the parallel charge/discharge effect upon the batteries electrical behaviour.

The level n° 5 was applied with for consequence a recharge factor near to 1.05. The table 1 groups together the main results about the applied test conditions. These values are valid up to cycle 8000. After this, the depth of discharge was reduced from 27% to 23%.

The first results show that the values are reproducable from one battery to an other; secondly, the battery voltages at all the key points during a cycle stayed stable apart from the end of the second discharge stage battery voltage (point E') for the peak power simulation (SPOT load profile) where we can apply an evolution law as follows:

$$U = Uo + mN$$

with N = cycle number

Uo and m were determined by a regression method (see table 2). The end of discharge voltage (point F') varied strongly and periodically without the possibility to develop an equation expressing the trend of U_{eod} with cycle number. The energy efficiency was greater than 80% which was one of the requirements for this type of LEO missions (fig. 7).

The cell temperatures appeared nearly the same for the three batteries, but nevertheless with a great dispersion which did not allow to provide an evolution law.

RESULT ANALYSIS FOR THE HYBRID TESTS

The test conditions are summarised in the table 3. The test has performed 7000 cycles without interruption. An interesting parameter is the battery voltage dispersion and the charge time at constant current (table 4). From the test results we can determine three evolution laws giving the time in function of the cycle number. Apparently most of the key points indicated no change during the 7000 cycles, only the point F' (end of discharge battery voltage) showed a linear decrease during the cycling (fig. 8 and table 5).

The battery temperatures showed a significant variation between the three batteries, at all stages during a cycle (table 6).

RESULTS ANALYSIS FOR THE REFERENCE TEST

As mentioned below, this test used the temperature derivative technique. Two series of cycles have been achieved:

-   First, two thousand cycles were performed with a very simple profile consisting of a charge at constant current until TDT detection followed by an open circuit for the end of charge period. Discharge was also at constant current (fig. 9). During this test phase, the K recharge factor has been constant and equal to 1.09. The DOD was around 26.2% and the energy efficiency fluctuated between 89 and 82%.

-   A second series of cycling was later carried out with the same profile as defined for the SPOT and Hybrid tests. The DOD was of 25.8% with a recharge factor of 1.11.

During the first six hundred cycles, the battery degraded linearly until a steady state was reached. Indeed, the end of discharge voltage decreased gradually from 1.30 volt to 1.15 volt; and then remained steady. The average end of discharge battery voltage was of 16.2 V with σ equal to 0.4 volt. Furthermore, we didn't see notable evolution of the charge time at constant current for the 5000 cycles (fig. 10). The average amplitude of temperature per cycle for the Reference test was lower than for the SPOT and Hybrid tests (table 7).

Although the energy efficiency remained almost constant during the cycling, a slight decrease in both the charge and discharge energies appeared after cycle 3800.

EVOLUTION LAWS

Equations which describe the variations of voltage and temperature with the cycling time are shown below. From the first series of results of the reference test we have tried a similar approach to that used to describe chronopotentiometry. Two cases have been studied.

- "Fast" systems where the interfacial concentrations are in a balance stage, we introduce the term "T_i" transition time where the concentrations $C(0, T_i) = 0$;

  therefore;

$$E = E^\circ + \frac{RT}{nF} \ln \frac{D_r^{\frac{1}{2}}}{D_o^{\frac{1}{2}}} \ln \frac{RT}{nF} + \frac{T_i^{\frac{1}{2}} - t^{\frac{1}{2}}}{t^{\frac{1}{2}}}$$

Where D_o and D_r are the diffusion coefficients of oxidising and reducing species respectively and t is the redox reaction time.

- With the second case, "slow" systems, we employ the classical cinetic law:

$$E = \frac{RT}{h \, naF} \ln \frac{T_i^{\frac{1}{2}} - t^{\frac{1}{2}}}{T_i^{\frac{1}{2}}} + \frac{RT}{h \, naF} \ln \frac{nFK^\circ Co^\circ}{i}$$

with   h = transfer coefficient
        na = electron number exchanged in the redox reaction
        k° = transfer speed

Therefore, two different laws have been tried:

1) $U = A + K \ln \dfrac{T_i^{\frac{1}{2}} - t^{\frac{1}{2}}}{t^{\frac{1}{2}}}$ (model 1)

2) $U' = A' + K' \ln \dfrac{T'_i^{\frac{1}{2}} - t^{\frac{1}{2}}}{T'_i^{\frac{1}{2}}}$ (model 2)

The parameters have been determined with the first series of results of the reference test for which the power profile was the simplest. It appears that the first model is better adapted for the charge mode whereas the second is better for the discharge phase. (fig.11)

During the cycling, T_i and K from equation 2 were found to decrease on discharge whereas on charge using equation 1, T_i increased whilst K decreased (fig. 13). Because of the more complicated discharged profile the models were inapplicable for the second series of the reference test as well as the SPOT and Hybrid tests. Indeed, the large random variations found in T_i and K confirm that such an approach is correct only when charge and discharge are carried out at constant current.

Concerning the curves of temperature versus time, it was found that the temperature was proportional to $1/\sqrt{t}$ for the charge period, whereas it was proportional directly to time on discharge. No variations due to ageing were discernable.

CONCLUSION

The main results are summarized in table 7. The results coming from the SPOT tests showed that most of the electrical performances of the three batteries were similar. The end of discharge battery voltage fluctuations are certainly due to a thermal unbalance of the batteries during cycling. This indicated that the main factor to be considered for a parallel charging system is the thermal environment of the batteries.

The Hybrid test presented less fluctuations in the end of discharge battery voltage from cycle to cycle than the SPOT test. Charging the three batteries separately has stabilized their appropriate recharge factor.

Indeed the Hybrid-test results showed a linear decrease of the battery voltage (Point F', fig 8) during the cycling from 17 volts to 14 volts, or less for the Battery 2 where the k recharge factor was the lowest (K = 1.04). The SPOT test results showed a general fluctuation of U_{eod} between 18 and 14 volts.(fig.14). The reason for this instability seemed due to a too low applied recharge factor.

The Reference test gave for the first time, results confirming that the Temperature Derivative Technique (TDT) seems a suitable one for charging batteries in LEO. Indeed, the main criterion for a good battery management system is to maintain the end of discharge cell voltage as high as possible and with minimum variation . this situation has been observed during the cycling where the battery voltage reached the average value at end of discharge of 16 volts (fig. 15 and table 7).

It is clear that the TDT method presents some advantages in comparison with the "standard" management because its principle is directly related to the reactions occuring in the batteries at end of charge. In another hand, the TDT stops the charging where batteries are charged and avoids any overcharge whatever the DOD profile is in operation; that is a major interest for lifetime.

We can mention that a similar test is running at the Battery Test Center at ESTEC with three batteries of 14 V035M cells each charged and discharged in parallel and managed by the Temperature Derivative Technique at 15 °C. Presently about 6000 cycles have been carried without problem. The end of charge and end of discharge cell voltage remain stable with the respective values:1.48 volt and 1.20 volt.

It is sure that all the tests described have been carried out with "commercial cells" (with the same type of electrodes used for the space cells), but nevertheless the comparison between the different charge techniques remain valid.

If the TDT method appears very attractive, it still presents some incertainties for a space application such as:

-     interferences between battery dissipation and external heat
      sources like solar radiation, battery heaters, ...

-     its behaviour under orbital conditions requiring the battery
      power during a part of the sunlight period, or with variable
      DOD and discharge at constant power instead of constant current
      as used in the above mentioned tests.

The use of mathematical models in order to represent the cell evolution in cycling is limited to the simple charge and discharge profiles such as the ones for the Reference test (first series).

REFERENCES

(1) ESTEC Contract n° 4999/82 - F DD

(2) ESA Patent/1.2/MM/6838 (H.J. Spruijt)

Table 1. SPOT TESTS CONDITIONS

Spot-Tests	Battery A	Battery B	Battery C
$\overline{Q_D}$ Ah	9.66	9.54	9.23
σ	0.35	0.32	0.28
$\overline{Q_C}$ Ah	10.19	9.96	9.54
σ	0.44	0.39	0.33
$\overline{K}$	1.05	1.04	1.035
σ	0.03	0.03	0.03
DOD %	27.6	27.3	26.4
σ	1	0.9	0.8

Table 2. EVOLUTION LAWS FOR THE SECOND DISCHARGE STATE BATTERY VOLTAGE (SPOT TESTS) WITH N = CYCLE NUMBER

(Volts)	COR.C
Battery A : $U_{F'A} = 17.53 - 5.7.10^{-4}$ N	- 0.624
Battery B : $U_{F'B} = 17.47 - 4.2.10^{-4}$ N	- 0.521
Battery C : $U_{F_C} = 17.42 - 3.1.10^{-4}$ N	- 0.398

Evolution Laws for the second Discharge Stage Battery Voltage (SPOT tests)

WITH N = CYCLE NUMBER

Table 3. HYBRID TESTS CONDITIONS

Hybrid Tests	Battery 1	Battery 2	Battery 3
$\overline{Q_D}$ Ah	9.42	9.48	9.72
σ	0.15	0.2	0.2
$\overline{Q_C}$ Ah	10.08	9.87	10.52
σ	0.15	0.3	0.2
$\overline{K}$	1.07	1.04	1.08
σ	0.02	0.03	0.02
DOD %	26.9	27.1	27.7
σ	0.4	0.6	0.6

Table 4. EVOLUTION LAWS FOR THE CHARGE TIME AT CONSTANT CURRENT
(HYBRID TESTS)

(hour)	COR. C
Battery 1 : $t = 0,543 - 16,2.10^{-6} N$	-0.904
Battery 2 : $t = 0,573 - 40,2.10^{-6} N$	-0.981
Battery 3 : $t = 0,580 - 8,8.10^{-6} N$	-0.610

Table 5. EVOLUTION LAWS FOR THE END OF DISCHARGE BATTERY VOLTAGE
(HYBRID TESTS) WITH N = CYCLE NUMBER

(volt)	COR. C
Battery 1 : $UF'_1 = 16,66 - 2,4.10^{-4} N$	-0.658
Battery 2 : $UF'_2 = 16,75 - 3,8.10^{-4} N$	-0.981
Battery 3 : $UF'_3 = 16,69 - 2,5.10^{-4} N$	-0.610

Table 6. AVERAGE IN CELL TEMPERATURES FOR THE HYBRID TEST

KEY POINTS	A''		B''		C''		D''		E''	
	$T(°C)$	σ	$T(°C)$	σ	$T(°C)$	σ	$T(°C)$	σ	$T(°C)$	σ
BAT 1	24.2	0.7	24.7	0.8	27.3	0.7	27.5	0.6	24.2	0.7
BAT 2	23.8	0.8	24.2	0.8	26.9	0.7	27.1	0.7	23.8	0.8
BAT 3	24.8	0.7	25.3	0.7	28.0	0.7	28.1	0.7	24.7	0.8

Table 7. GENERAL RESULTS FOR THE THREE TESTS

TESTS	SPOT			HYBRID			REFERENCE
DOD %	27.6	27.3	26.4	26.9	27.1	27.7	25.8
K_F	1.05	1.04	1.035	1.07	1.04	1.08	1.11
V_{eoc} (volt)		1.408		1.416	1.408	1.421	1.484
$\overline{U_{eod}}$(volts)	Fluctuations between: 18 volts and 13.9 volts			From: 17 volts to 14 volts			16 volts
W_c kJ	704	693	667	709	706	765	698
W_d kJ	602	597	588	579	577	588	563
η %	86	86	88	82	82	77	81
Δ °C		3.2			3.3		2.8
BATTERIES	A	B	C	1	2	3	1 battery

Figure 1. Diagram of the Packaging
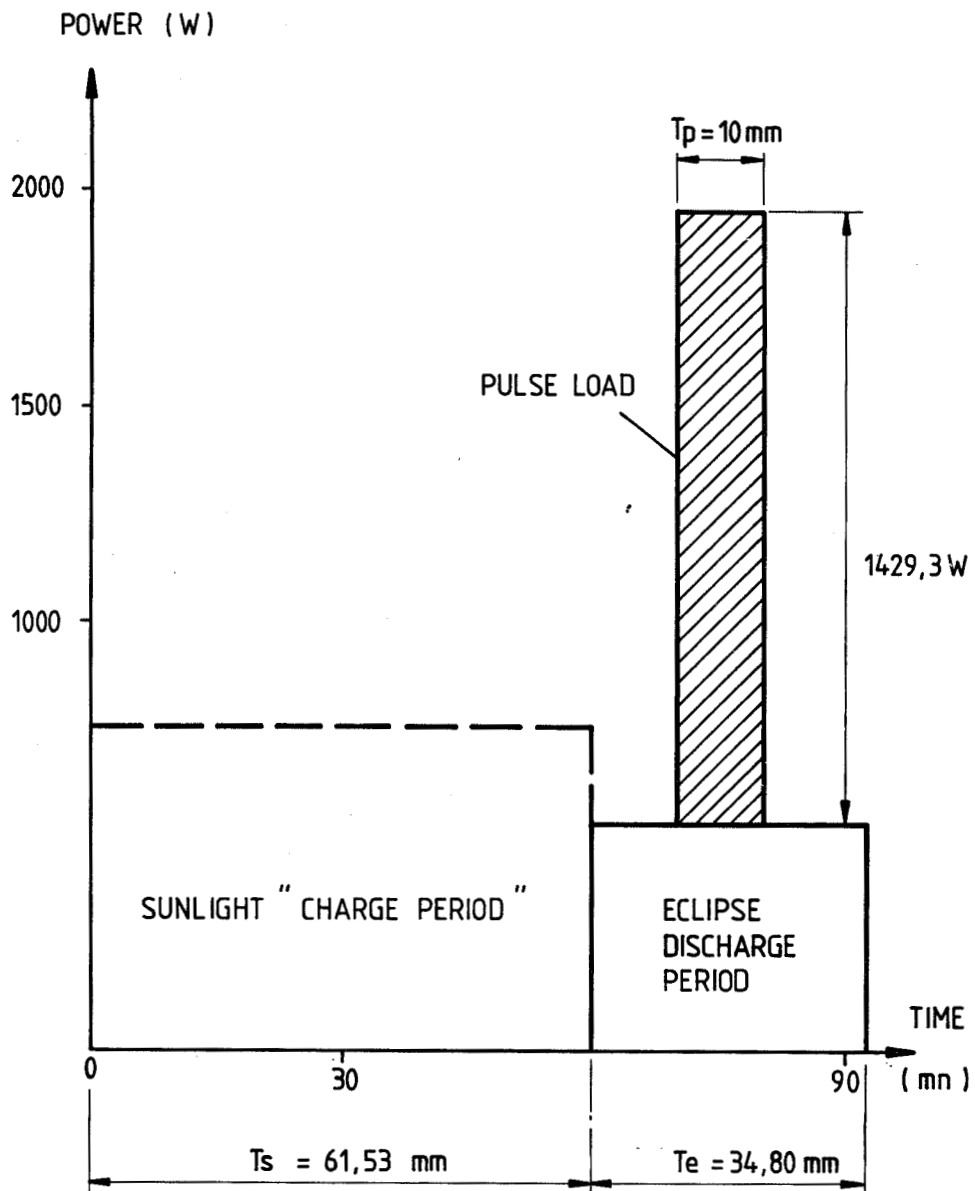
Figure 2. SPOT Power Profile
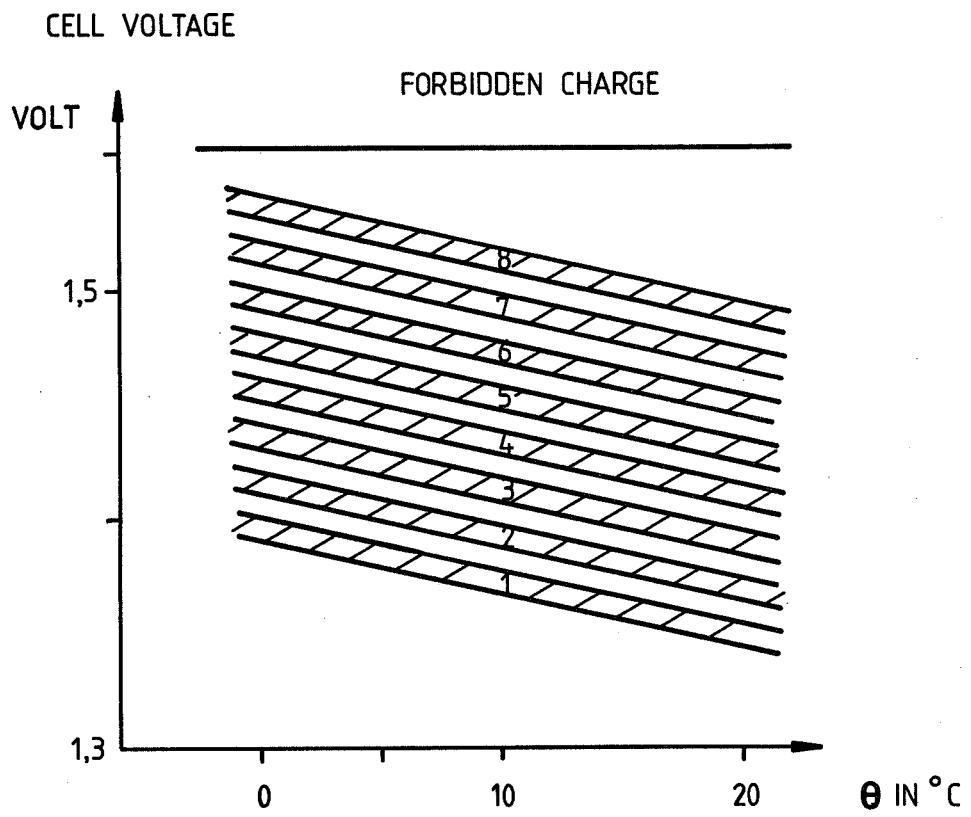
Figure 3. Voltage Limit Function of Temperature
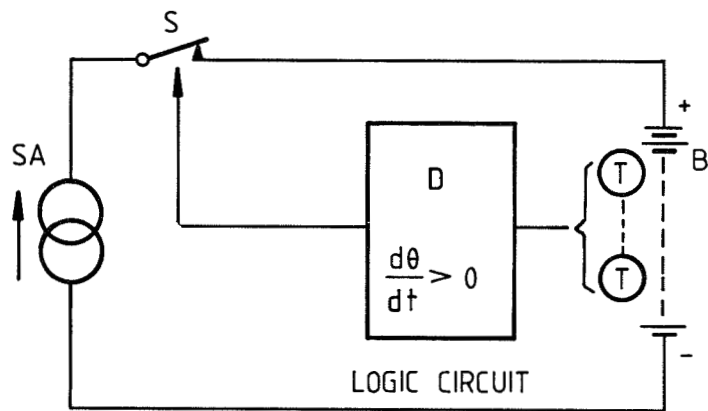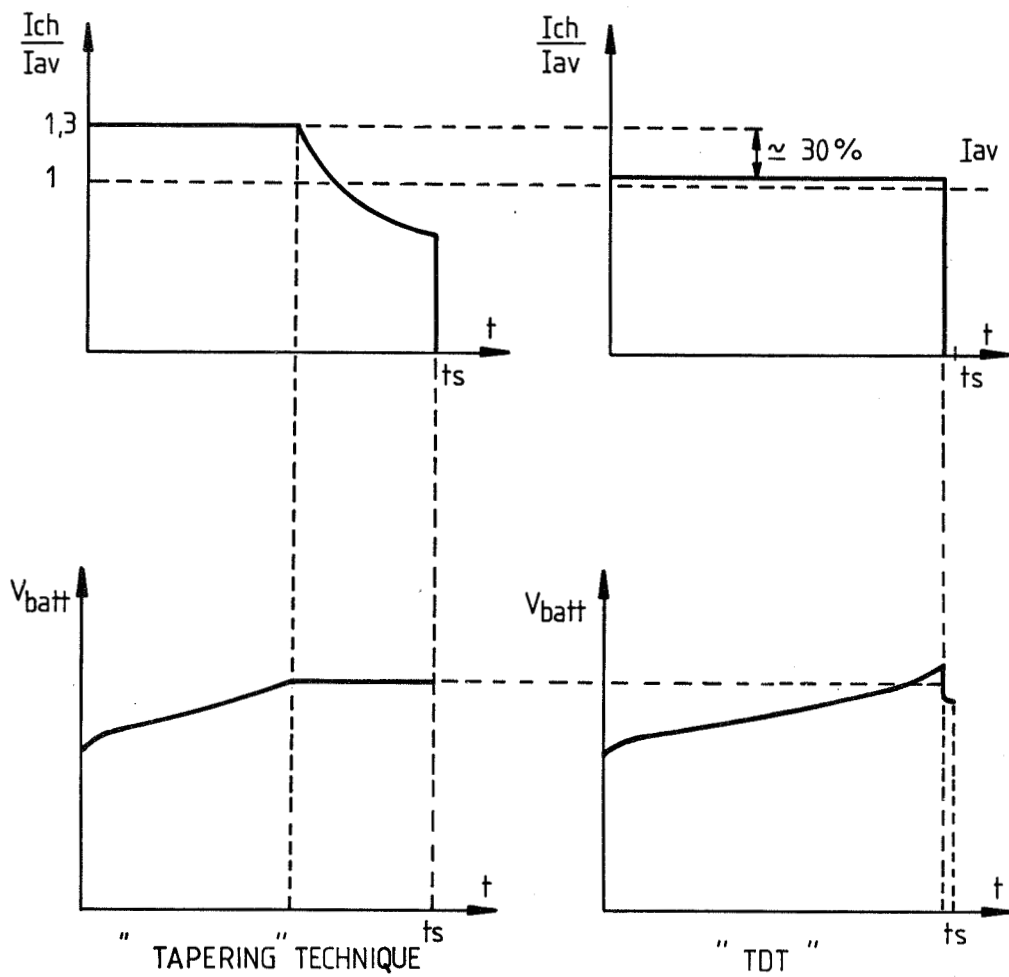
Figure 4.
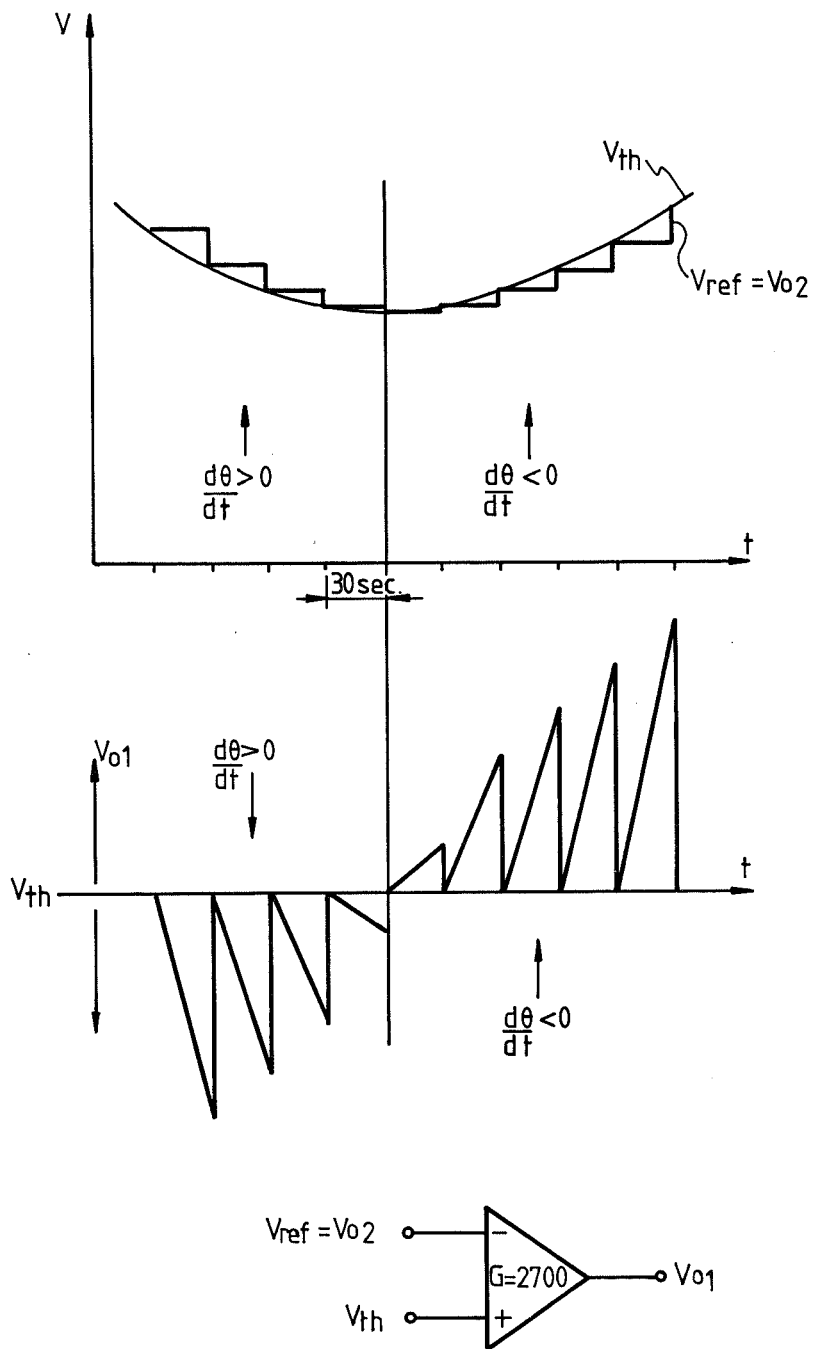
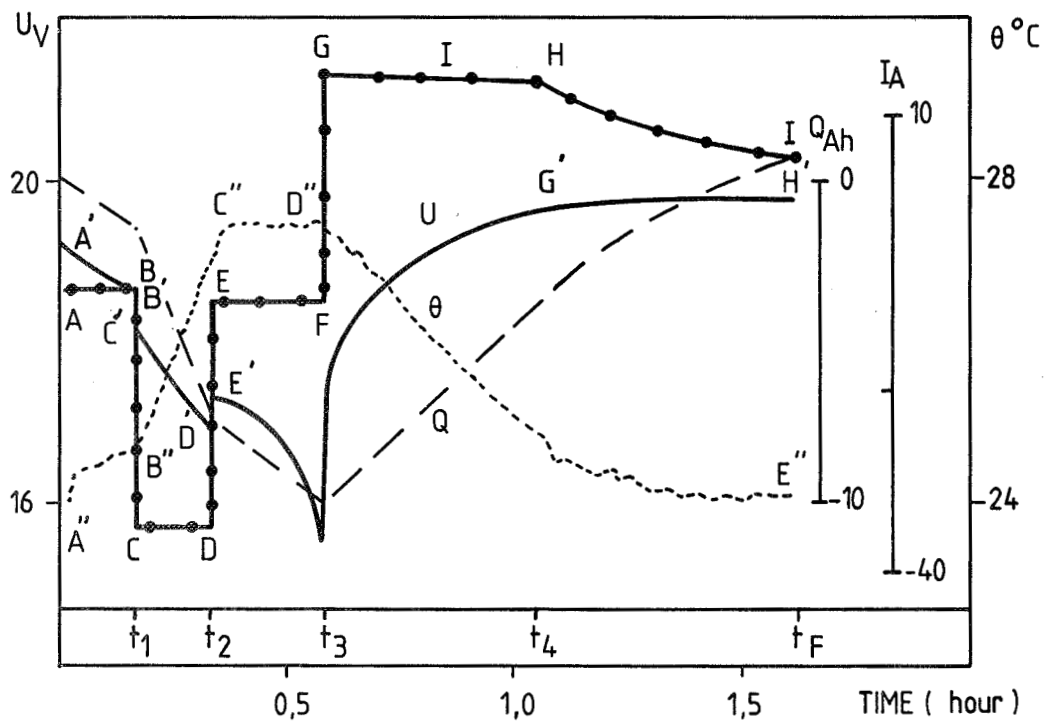Figure 5. Temperature Derivative Technic Principle
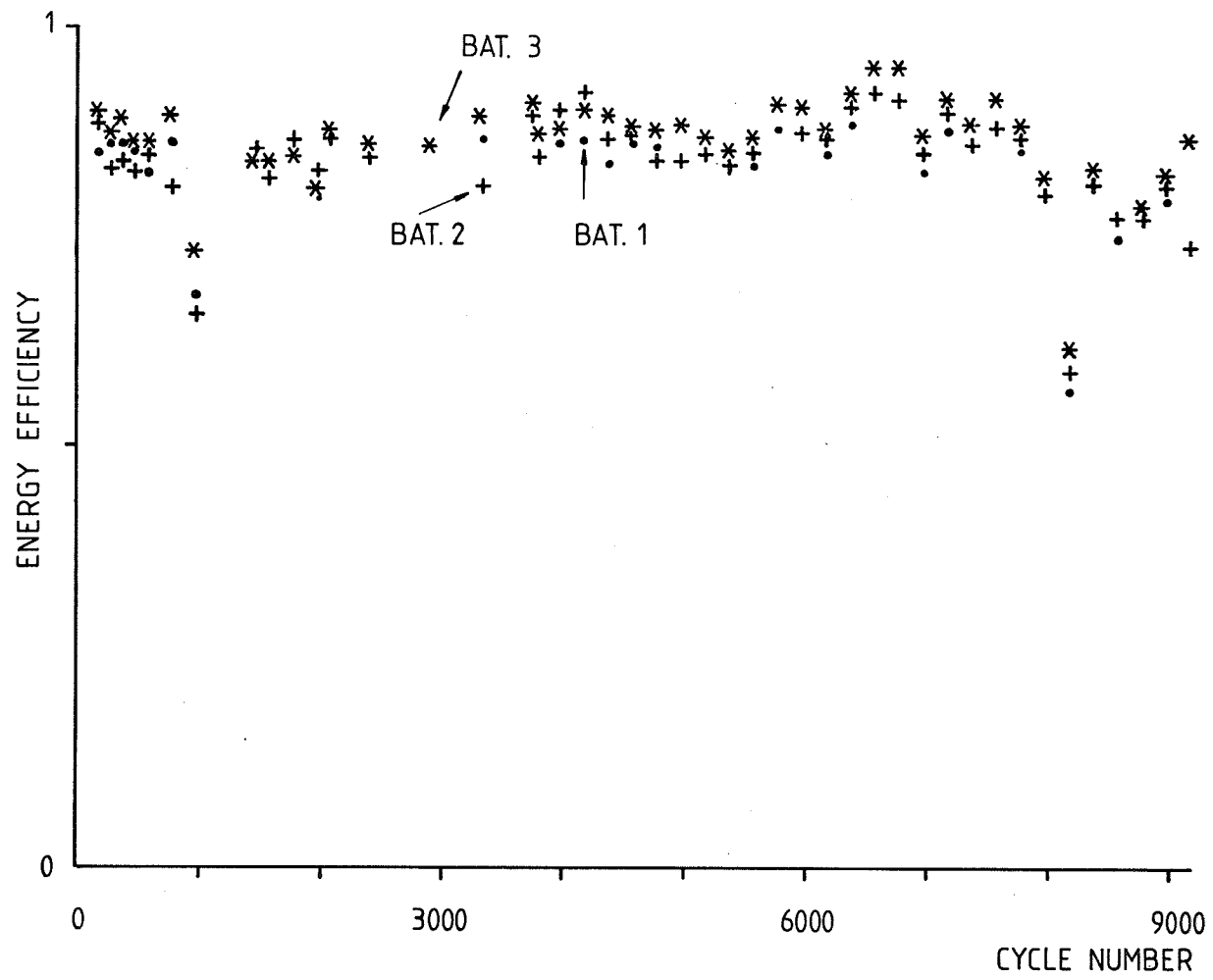
Figure 6. SPOT Tests Description
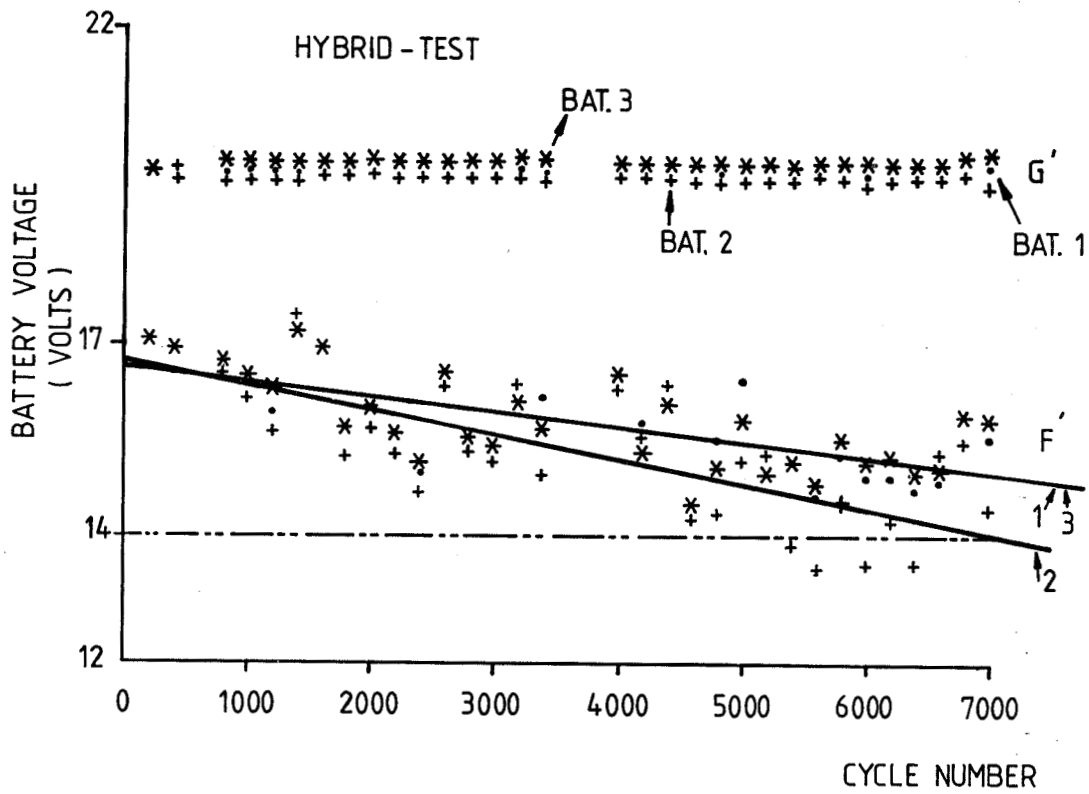
Figure 7. SPOT Tests

Figure 8. Battery Voltage Evolution at the End of Charge (Point G') and End of Discharge (Point F') in Function of the Cycle Number
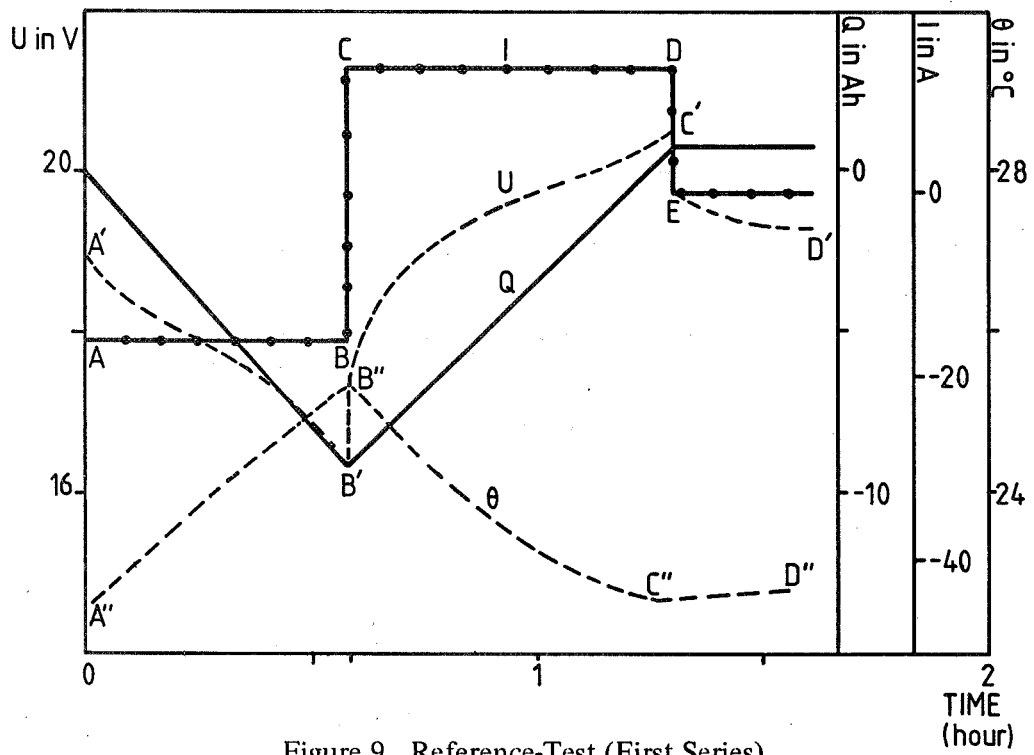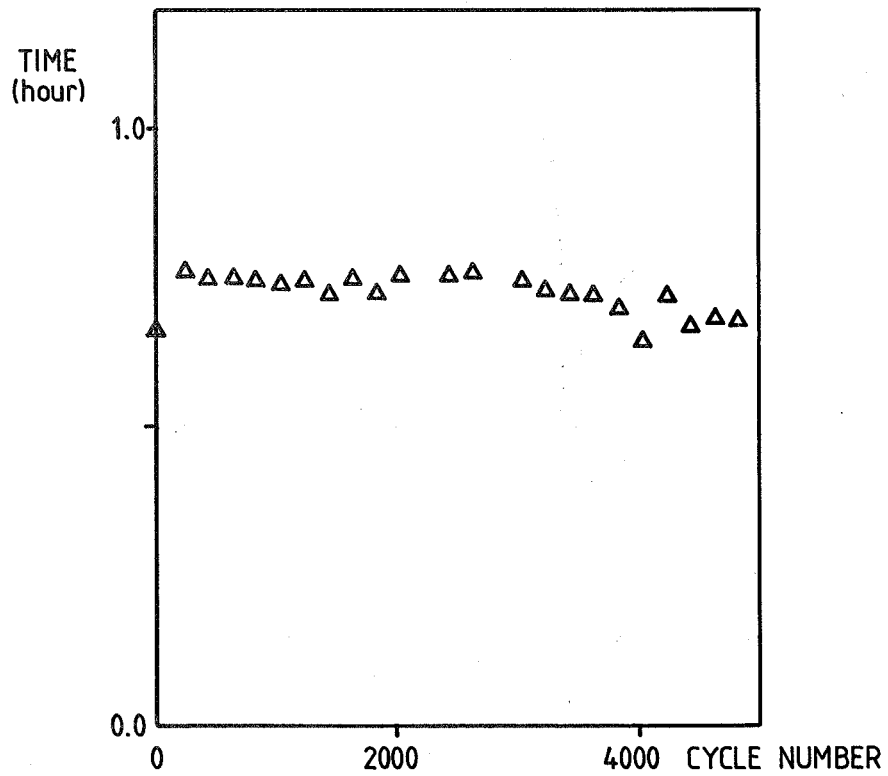
Figure 9. Reference-Test (First Series)

Figure 10. Reference-Test (Second Series) Charge Time
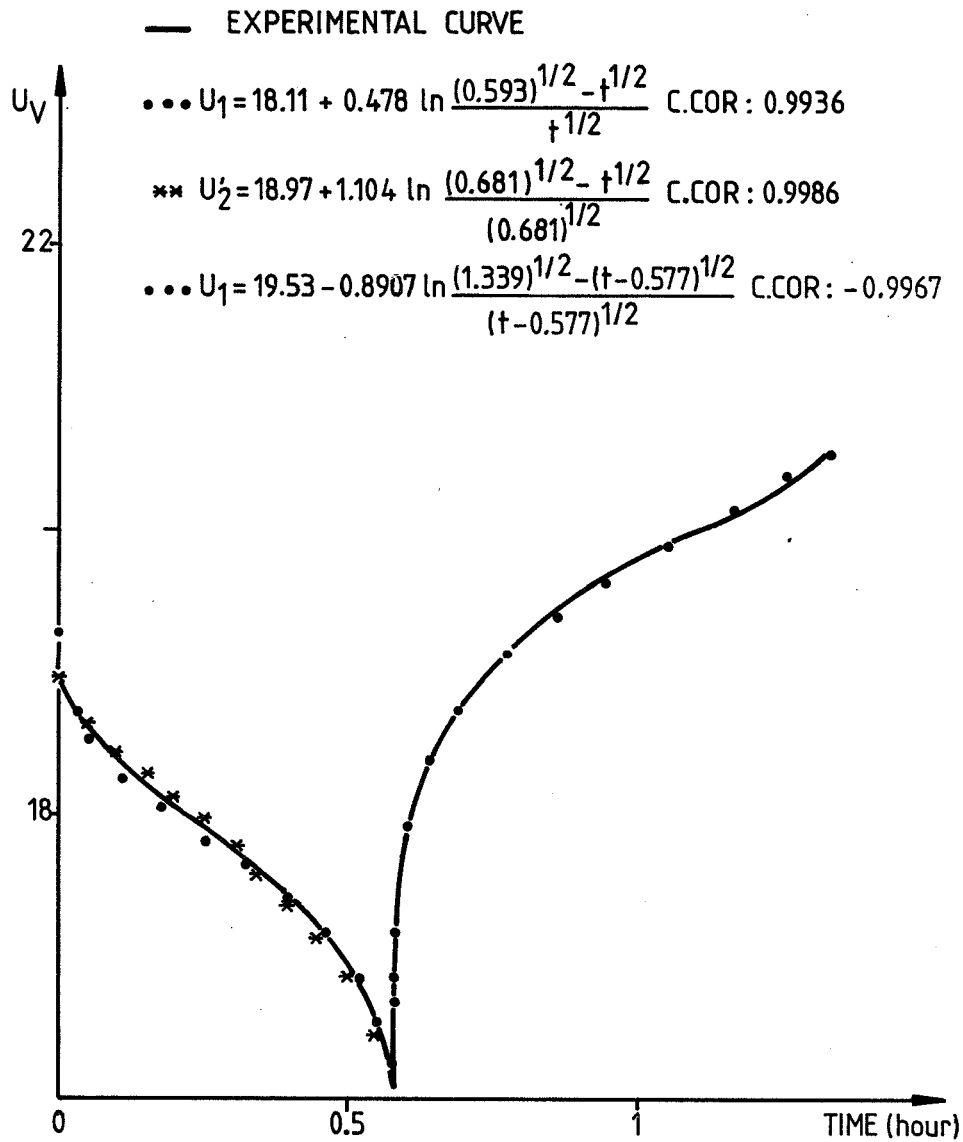at Constant Current

362

EXPERIMENTAL CURVE

$U_1 = 18.11 + 0.478 \ln \dfrac{(0.593)^{1/2} - t^{1/2}}{t^{1/2}}$ C.COR : 0.9936

$U_2' = 18.97 + 1.104 \ln \dfrac{(0.681)^{1/2} - t^{1/2}}{(0.681)^{1/2}}$ C.COR : 0.9986

$U_1 = 19.53 - 0.8907 \ln \dfrac{(1.339)^{1/2} - (t - 0.577)^{1/2}}{(t - 0.577)^{1/2}}$ C.COR : -0.9967

U_V

22

18

0   0.5   1   TIME (hour)

Figure 11; Reference-Test (First Series), Cycle 1000

Cronopotentiometric Models for the Battery Voltage
for Charge and Discharge Periods

363
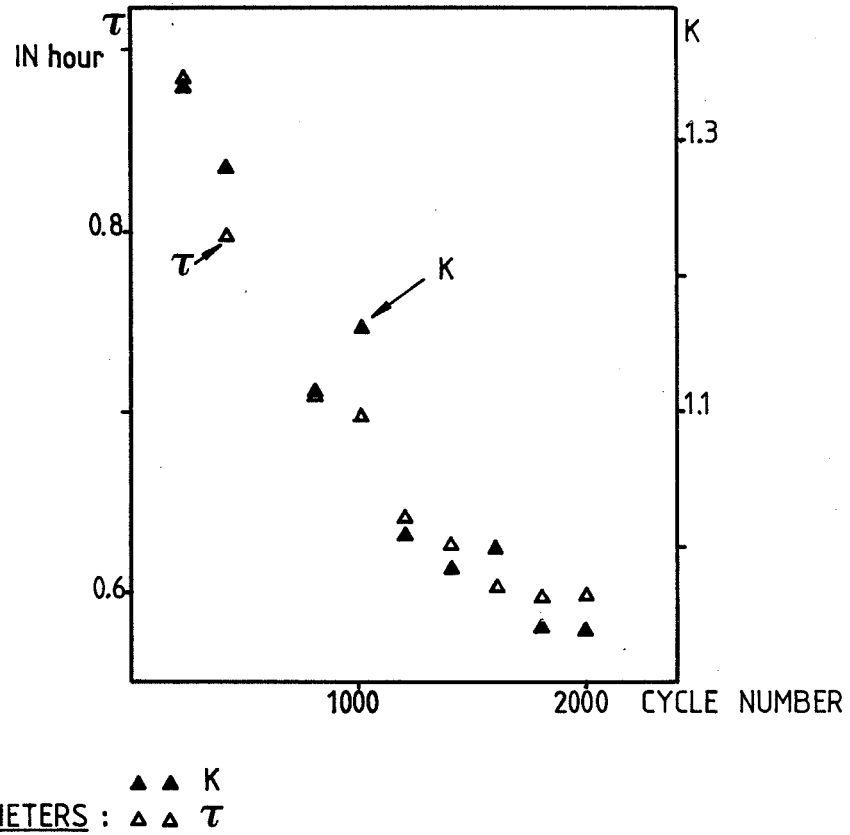
Figure 12. Reference-Test (First Series) τ and K Evolution in Function of the Cycle Number for the Discharge Period
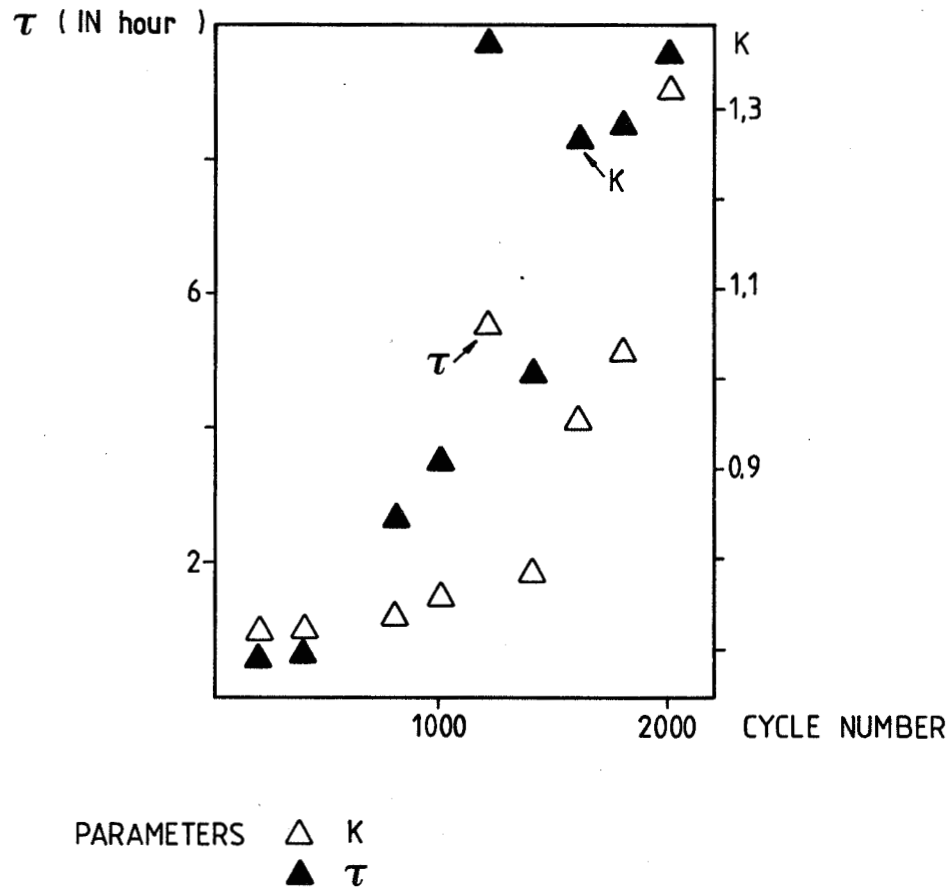
Figure 13. Reference-Test (First Series) τ and K Evolution in Function
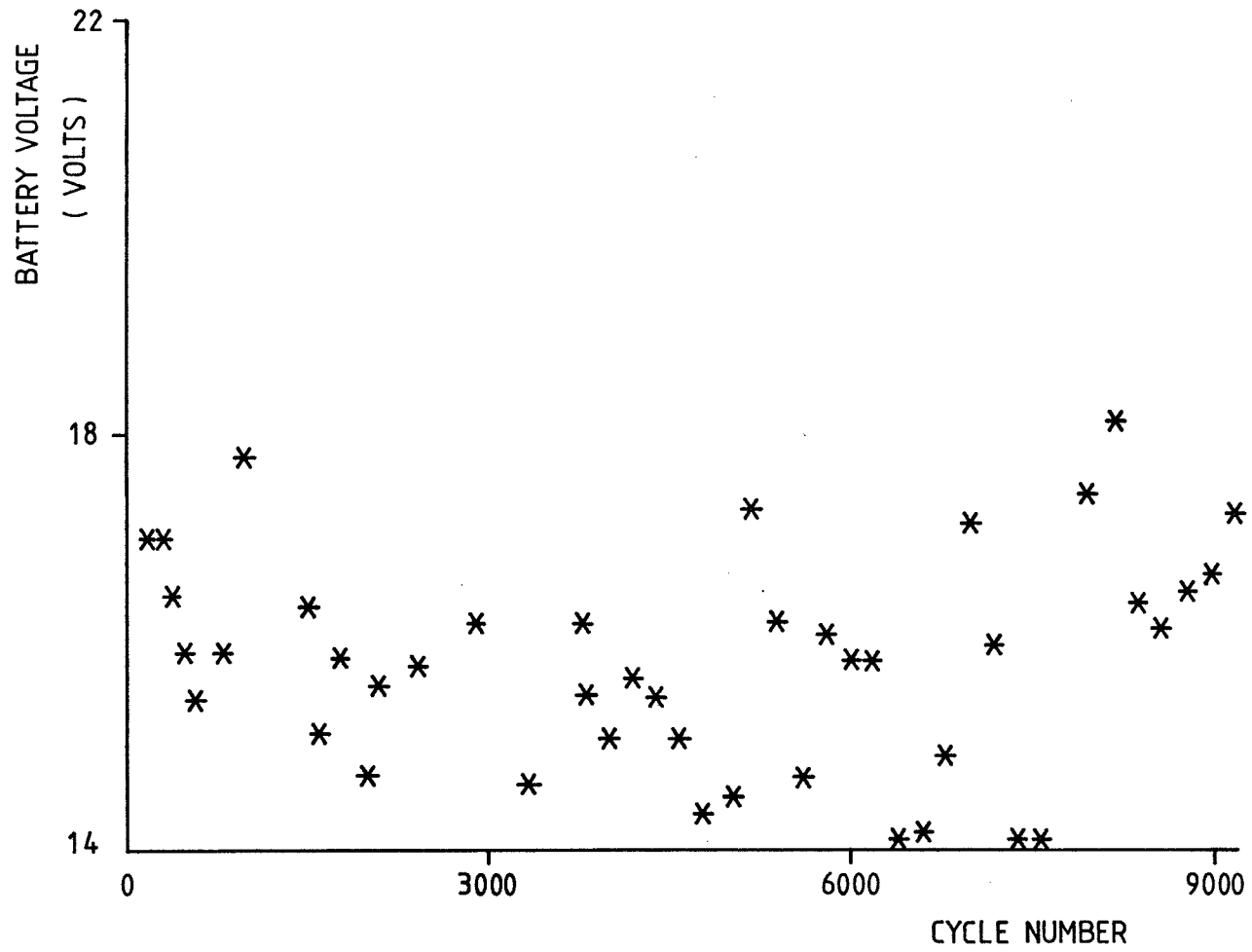of the Cycle Number for the Charge Period

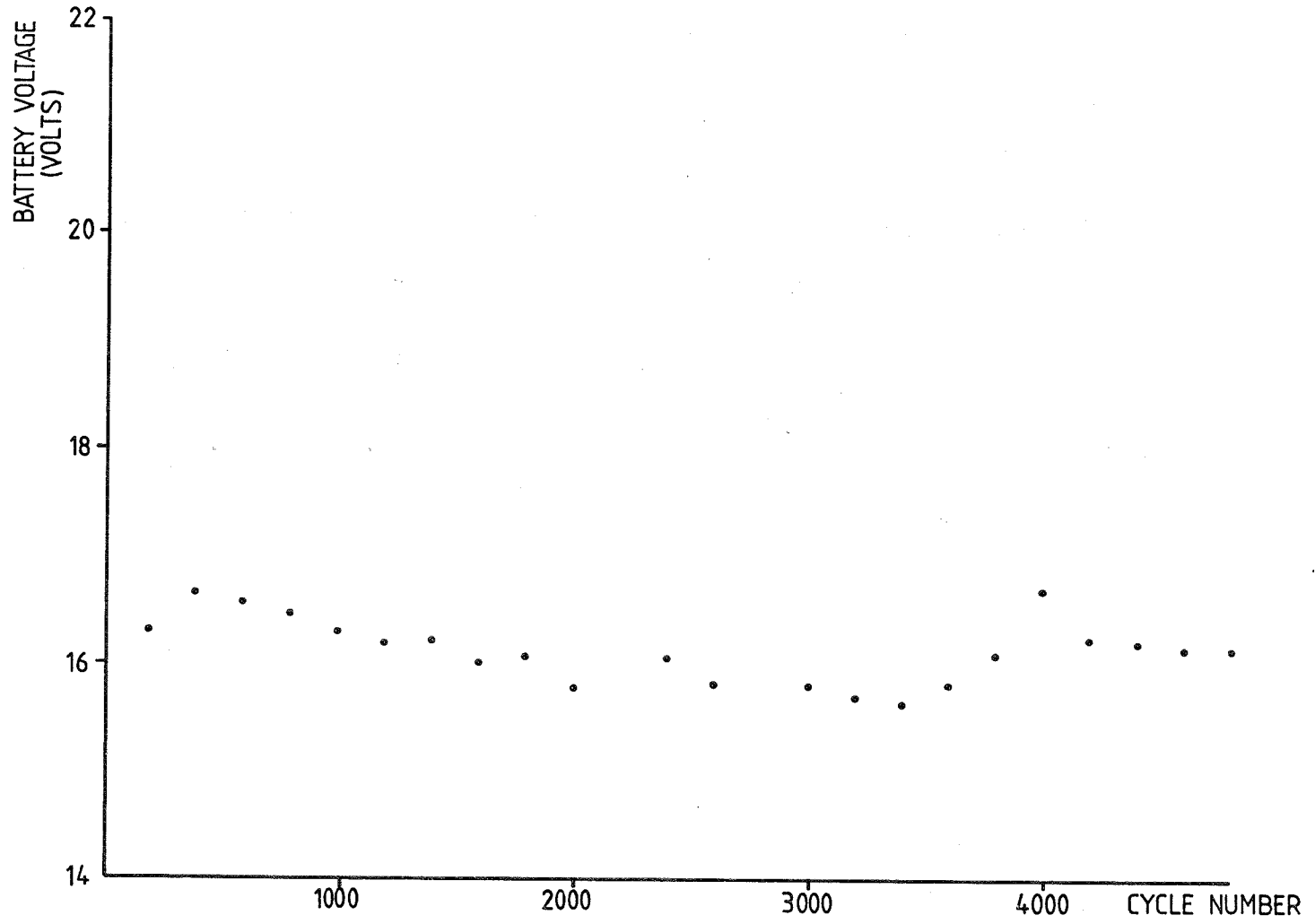Figure 14. Spot-Test, End of Discharge Battery Voltage (Point F′)

Figure 15. Reference-Test (Second Series), End of Discharge Battery Voltage Evolution